Sorting Stable versus Unstable Hypothetical Compounds: The Case of Multi-Functional ABX Half-Heusler Filled Tetrahedral Structures

*Xiuwen Zhang, Liping Yu, Andriy Zakutayev, and Alex Zunger**

Electronic structure theory has recently been used to propose hypothetical compounds in presumed crystal structures, seeking new useful functional materials. In some cases, such hypothetical materials are metastable, albeit with technologically useful long lifetimes. Yet, in other cases, suggested hypothetical compounds may be significantly higher in energy than their lowest-energy crystal structures or competing phases, making their synthesis and eventual device-stability questionable. By way of example, the focus here is on the family of 1:1:1 compounds ABX called "filled tetrahedral structure" (sometimes called Half-Heusler) in the four groups with octet electron count: I-I-VI (e.g., CuAgSe), I-II-V (e.g., AgMgAs), I-III-IV (e.g., LiAlSi), and II-II-IV (e.g., CaZnSn). First-principles thermodynamics is used to sort the lowest-energy structure and the thermodynamic stability of the 488 unreported hypothetical ABX compounds, many of which were previously proposed to be useful technologically. It is found that as many as 235 of the 488 are unstable with respect to decomposition (hence, are unlikely to be viable technologically), whereas other 235 of the unreported compounds are predicted to be thermodynamically stable (hence, potentially interesting new materials). 18 additional materials are too close to determine. The electronic structures of these predicted stable compounds are evaluated, seeking potential new material functionalities.

1. Introduction

The quest for physically interesting and potentially technologically useful functional materials has recently propelled numerous proposals of hypothetical materials with exciting properties promised by first-principles calculations. Some examples include "harder than diamond" carbon-nitrides,[1] the room-temperature oxide ferromagnets,[2] the new Li battery materials,[3] Half-Heusler piezoelectrics,[4] the honeycomb-structured topological insulators,[5] direct bandgap Si-Ge superlattices,[6] and Half-Heusler optoelectronic materials.[7] Some of these hypothetical materials are metastable, but metastability is not a concern if the hypothetical structure is both locally stable and is protected from fast decay into the lowest-energy structure by practically insurmountable activation barriers. For example, semiconductor superlattices and quantum-wells (AC)/(BC) made of the binary constituent semiconductors AC and BC may be ≈10–40 meV per atom higher in energy (similar to energy difference between graphite and diamond) than the AC + BC phase-separated system,[8a,8b] yet such (AC)/(BC) structures can have very long and technologically useful lifetimes.[8c] Experimental synthesis techniques based on high-energy reactants[8d] have routinely produced metastable, long lived compounds such as Na_3N[8d] or nitrogen-doped ZnO[8e] all corresponding to positive formation enthalpies. However, prediction of technologically useful properties of 3D, metastable inorganic materials is largely irrelevant if a hypothetical compound is not protected from rapid decay into the lowest energy. Some examples include proposed new compounds that are, in fact, dynamically unstable in the proposed structure, such as zincblende ferromagnets[9] or zinc blende PtN (proposed in ref. [10a] and discussed in ref. [10b]). A list of dynamically unstable hypothetical binary compounds, including AlP, AlAs, GaP, GaAs, AlSb, GaSb, and InSb in the NaCl structure, and ZnO, CdO, HgO, AlN, GaN, InN, InP, and InAs in the beta-Sn structure was provided in ref. [10c,d]. These phases many have interesting physical properties, but they do not exist.

1.1. The Challenge of Missing Ternary Materials

Proposed hypothetical ternary or multinary materials feature prominently in the theoretical literature on new compounds,[1–10] but many theoretical papers in this field focus on

Dr. X. Zhang
Colorado School of Mines
1500 Illinois Street, Golden, CO 80401, USA
Dr. L. Yu, Dr. A. Zakutayev
National Renewable Energy Laboratory
1617 Cole Blvd., Golden, CO 80401, USA
Prof. A. Zunger
University of Colorado
914 North Broadway Street
Boulder, CO 80309, USA
E-mail: alex.zunger@gmail.com

DOI: 10.1002/adfm.201102546

interesting properties of ternary compounds that may not exist in the proposed structures or may be unstable with respect to disproportionation.[4,5,7] ABX materials with presumed AgMgAs-type (filled tetrahedral) crystal structure, also known as "Half-Heuslers" were recently considered.[4,7] For example, piezoelectric properties of ≈800 materials with electron count (EC) 8 and EC = 18 have been calculated in the hypothetic Half-Heusler AgMgAs-type structure.[4] Also, some topological insulator properties of 24 ABX compounds were calculated in the hypothetic ZrBeSi-type structure,[5] and optoelectronic properties of ≈600 EC = 8 ABX compounds have been calculated in the assumed Half-Heusler AgMgAs-type structure.[7] In all these cases the stability of the proposed materials with respect to disproportionation has not been addressed in detail. In general ABX ternary materials can manifest instability with respect to decomposition into any combination of elemental or binary constituents leading to the prospects of spontaneous disproportionation or even to difficulty of making the ternary material in the first place. Therefore, the absence of many recently proposed ABX hypothetical ternary materials from the crystallographic databases[11] poses an interesting question: Are these missing ternary materials thermodynamically unstable, or are they missing because no one has attempted to synthesize them as of yet? The answer to this question would help to determine which of these proposed hypothetical ternaries have an opportunity to become new useful functional materials. Determining the lowest-energy structure of a material and its thermodynamic stability with respect to decomposition into combination of binaries is an important step towards this goal.

In this paper, we use first-principles thermodynamics based on density-functional methodology to calculate the stability of the unreported 488 ternary ABX compounds including I-I-VI, I-II-V, I-III-IV, and II-II-IV groups with electron count of 8. The merit of considering the octet rule for the set of ABX compounds is that the possibility of finding a stable compound is much higher (48%) than without forcing octet rule (<25%).[12] Out of 488 compounds that were previously not reported in the Inorganic Chemistry Structural Database (ICSD)[11a,11b] and the powder diffraction file (ICDD PDF)[11c] 235 are found here to be unstable with respect to decomposition and 18 are too close to call. On the other hand, we find 235 thermodynamically stable ABX compound and sort their crystal structures. Furthermore, the bandgaps and absorption spectra are calculated based on "GW theory"[13] for these stable compounds in their lowest-energy structure suggesting the potential material functionalities. This opens the door to identification of interesting and hitherto unreported new functional materials.

2. Classification of ABX Half-Heusler Compounds Built Upon the Filled Tetrahedral Structure

The zinc blende lattice, with a cation at site T1 = (0,0,0) and anion at site T2 = (¼,¼,¼) are extremely "open" structures, having ≈66% of the unit cell volume empty (if the two atoms have touching sphere radii). The filled tetrahedral structures (FTS)[14] can be created by partial or full occupation of the two empty tetrahedral interstitial sites IT1 = (½;½;½) and IT2 = (¾,¾,¾), where numbers in parentheses are Wyckoff position of atoms in the cubic cell with the origin at (0,0,0). By stuffing an atom at IT1 (surrounded by four anions at T2), and/or stuffing an atom at IT2 (surrounded by four cations at T1) one can generate a half-FTS, or full-FTS, respectively. Based on the character and location of the stuffing atom, the FTS can be divided in the five classes (**Table 1**). These five classes result from i) stuffing a cation (usually on IT1), ii) stuffing an anion (usually on IT2) (half-FTS), iii) stuffing a pair of cation/anion, iv) a pair of cation/cation, or v) a pair of anion/anion on both interstitial sites IT1/IT2 (full-FTS).

Table 1. The five classes of FTS.

Class	Closed-shell EC	Pearson Symbol
Cation stuffed	8, 18	cF12
Anion stuffed	16	cF12
Cation/anion stuffed	16	cF16
Cation/cation stuffed	8, 18	cF16
Anion/anion stuffed	24	cF16

The first class, cation-stuffed FTS, contains five groups with electron count of 8 as listed in **Table 2**: a) I-I-VI, e.g., CuAgSe; b) I-II-V, e.g., AgMgAs; c) I-III-IV, e.g., LiAlSi; d) II-II-IV, e.g.,CaZnSn; and e) II-III-III, e.g., MgAlY. This paper focus on the first 4 groups, because the II-III-III group has different chemical character.

The cation-stuffed FTS compounds are sometimes referred to as "Half-Heusler compounds", named after Heusler who studied Heusler alloys A_2BX in the early 20th century[15] (the compounds listed in Table 2 were not actually made by Heusler but instead by Nowotny, Juza, Hund et al.[11a,11b]). The driving forces to study cation-stuffed FTS compounds in the recent years were the possible thermoelectric,[16a,16b] magnetic,[16c,16d] optoelectronic,[14,17] and topological insulator[18] applications.

3. Methods

Figure 1 illustrates some of the burden-of-proof required to predict the existence of hypothetical multinary compounds. One faces two main problems. First, there is a question of the lowest-energy crystal structure of an unknown multinary compound. Second is the question of the stability of a given compound with respect to decomposition into its elemental,

Table 2. The five groups of cation-stuffed FTS with EC = 8.

Group	Reported compounds (examples in ICSD)
I-I-VI	CuAgSe, AuLiS, CuLiO
I-II-V	AgMgAs, LiZnP, LiZnN
I-III-IV	LiAlSi, LiGaGe, CuLaSn
II-II-IV	CaZnSn, MgSrSi, SrZnGe
II-III-III	MgAlY, MgGaY, MgInY

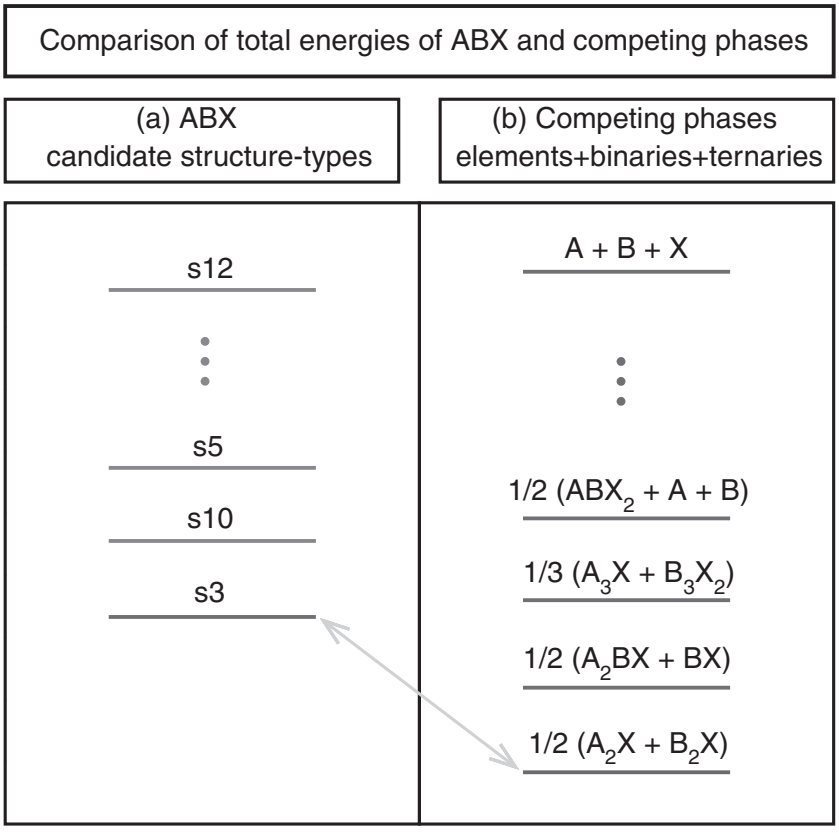

Figure 1. Schematic illustration of analyzing the thermodynamic stability of a hypothetical ABX compound by comparing a) its total energy in the lowest-energy structure with b) the sum of total energies of competing phases.

high-throughput approaches that examine a large number of potentially overlooked compounds.

Alternatively, one can construct a set of candidate structure types for a specific stoichiometry (e.g., 1:1:1 structure types are listed in Table 3), calculating their total energies using density functional theory (DFT)[22–24] and determining the structure with the lowest energy. Figure 2b illustrates the calculation of candidate structures of NaBaAs, which gives the lowest-energy structure being b4 in agreement with the GSGO results. There are dozens of higher-energy structures lying in the energy interval 100 meV per atom above the ground state energy for NaBaAs, in contrast to ZnCdSn whose lowest-energy structure is well separated from the higher-energy structures. The list of structure types in Table 3 is obtained from the crystal structures of existing compounds in 1:1:1 stoichiometry in the ICSD database.[11a,11b] This approach requires ≈100 independent total energy calculations per ABX compound, which is less computationally extensive (but also less certain because the correct structure may be unknown and not in the list) than most of the existing structure searching methods (e.g., GSGO, simulated annealing, topological modeling, and molecular packing[25]).

binary, ternary, and multinary competing phases. In this section we describe our approach to solving these two problems and the method to evaluate the electronic structure of stable compounds.

3.1. Determining the Lowest-Energy Structure of a Multinary Compound

The problem of the lowest-energy structure of a multinary compound can be solved successfully by applying the global space group optimization (GSGO) method,[19] that starts from the unbiased guess of randomly selected lattice vectors and random atomic positions within a (super) cell as input for a sequence of ab initio calculations of total energy of locally relaxed trial structures to search for a global minimum via an evolutionary-algorithm selection. This approach naturally produces low energy structures that are also assured to be dynamically stable. **Figure 2**a shows the GSGO history of NaBaAs.[20] The ground state structure found by GSGO for NaBaAs is the Fe_2P-type (s4) structure (**Table 3**). The GSGO method has been found to be successful in identifying interesting and often unsuspected crystal structures by us[19] and by other researchers.[21] However, GSGO typically requires significant computational resources to solve the lowest-energy structure of a single compound. It is not tractable within

3.2. Analysis of Thermodynamic Stability With Respect To Decomposition

A compound is considered stable under the thermodynamic equilibrium conditions if the values of the chemical potentials are such that the formation of a given hypothetical ABX compound is energetically the most favorable of all possible competing phases (Figure 1). Mathematically, this means that the following equality and a set of inequalities need to be satisfied simultaneously:

$$\Delta\mu_A + \Delta\mu_B + \Delta\mu_X = \Delta H_f(ABX), \quad (1)$$

$$\Delta\mu_I \leq 0,\ I = A, B, X, \quad (2)$$

$$n^{(i)}\Delta\mu_A + m^{(i)}\Delta\mu_B + q^{(i)}\Delta\mu_X \leq \Delta H_f(A_{n^{(i)}}B_{m^{(i)}}X_{q^{(i)}}),\ i = 1, ..., Z \quad (3)$$

where $\Delta\mu_I$ is the chemical potential of element I with zero-point at the total energy of the standard phase of the element, ΔH_f is the formation enthalpy, Z is the number of competing phases, and $n^{(i)} : m^{(i)} : q^{(i)}$ are the stoichiometries of the competing phases. Graphically, the equilibrium condition Equation (1) for a ternary compound gives a plane in the 3D space of chemical potentials. Each competing phase cuts off a part of the plane, as illustrated in **Figure 3**a,b for CaSrC and CuNaS, respectively.

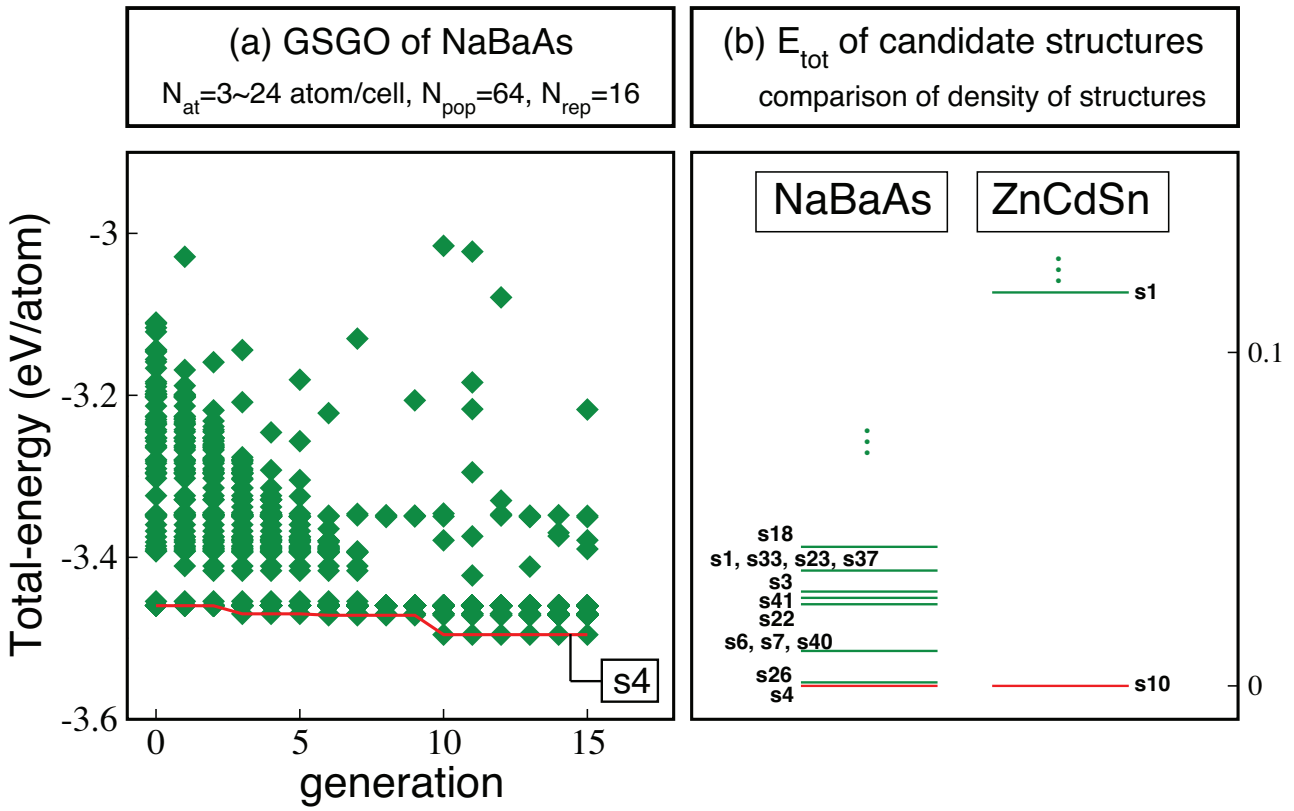

Figure 2. a) GSGO history of NaBaAs and b) total energies of candidate structure types of NaBaAs (left) and ZnCdSn (right).

If a part of the plane is left after considering all the competing phases, then the compound is thermodynamically stable, otherwise it is unstable.[26]

To study the possible decomposition of ABX ternary compounds into competing phases, one needs to calculate with relevant accuracy the formation enthalpies of both the compound under the investigation and its competing phases (Equation (1–3)). However, standard approximations to density functional theory (DFT), namely local density approximation (LDA) and generalized gradient approximation (GGA), are known to predict poorly the ΔH_f values of inorganic compounds.[27] One can determine a set of elemental-phase reference energies to optimally cancel the errors with the computed total energies,[24,27] so as to calculate the ΔH_f values with relevant accuracy.

3.3 Testing the Method for Known and Stable ABX

As a reference test for the method, we apply it to 20 ABX compounds previously synthesized and listed in ICSD[11a,11b] (BaZnSi, BaZnSn, CaZnGe, AgKO, KCaBi, CuKSe, KMgAs, KMgP, KZnSb, LiAlGe, LiAlSi, LiBeN, CuLiO, LiInGe, LiMgN, LiSrSb, LiYGe, NaAlSi, RbCaAs, and SrZnSi), involves both structure determination (Figure 1a) and triangle analysis (Figure 1b). Their thermodynamic stability is confirmed according to this method, giving us some confidence in the approach. The lowest-energy structures of these materials also agree with their experimentally reported crystal structures.[11a,11b] The limitation of our approach is that the new ternary compounds are tested for thermodynamic stability based on the information of known binary and ternary competing phases, while unknown possible competing phases are not considered.

3.4. Evaluation Method for Electronic Structure of Stable Compounds

Once we established stable compounds and their structurally optimized geometry, state-of-the-art electronic structure methods were applied to determine their optical properties. The bandgaps and absorption spectrums are calculated based on the GW approximation[13a] for electron's self-energy, which has been widely and successfully applied in first-principles quasiparticle electronic-structure calculations for real materials.[13b,13c,28] We have used the same Γ-centered homogeneous k-meshes ($k_1 \times k_2 \times k_3$), which are determined according to the lengths of lattice vectors ($\mathbf{a}_1, \mathbf{a}_2, \mathbf{a}_3$), i.e., k_i = 8, 6, 4, 2, 1 respectively for $|\mathbf{a}_i| < 4.5$ Å, 4.5 Å $< E_g^{df} <$ 7.5 Å, 7.5 Å $< |\mathbf{a}_i| <$ 9.5 Å, 9.5 Å $< |\mathbf{a}_i| <$ 16 Å, and $|\mathbf{a}_i| >$ 16 Å, where i = 1, 2, 3. In general, we chose the number of unoccupied bands in GW calculation at least 9 times of the number of occupied bands for a system with fewer than 40 atoms. For larger system that can be handled, we use 1280 total bands which usually contain at least 512 unoccupied bands. The direct optical forbidden gap E_g^{df}, and the direct optical allowed gap E_g^{da} are determined from the magnitude of matrix element square $|M|^2$. If $|M|^2 < 10^{-3}$ eV^2 Å^{-2}, the

Table 3. Structure types of 1:1:1 stoichiometry.

Label	Prototype Compound	Space Group	Pearson's Symbol/ Mineral Name
s1	AgMgAs	F-43m (216)	cF12
s2	LiGaGe	$P6_3mc$ (186)	hP6
s3	PbClF	P4/nmm (129)	tP6
s4	Fe_2P	P-62m (189)	hP9/Barringerite
s5	ZrBeSi	$P6_3/mmc$ (194)	hP6
s6	MgSrSi	Pnma (62)	oP12
s7	$PbCl_2$	Pnma (62)	oP12
s8	CoYC	$P4_2/mmc$ (131)	tP6
s9	AuLiS	C2/c (15)	mS24
s10	AuRbS	Cmcm (63)	oS12
s11	CuKO	I-4 (82)	tI24
s12	CuLiO	I4/mmm (139)	tI24
s13	CuBaN	C2/c (15)	mS36
s14	LiCaN	Pnma (62)	oP12
s15	BaNiN	Pnma (62)	oP36
s16	LiBeN	$P2_1/c$ (14)	mP12
s17	BaPtSb	P-6m2 (187)	hP3
s18	LiYSn	$P6_3mc$ (186)	hP24
s19	ScAuSi	P-6m2 (187)	hP6
s20	PtYAs	$P6_3/mmc$ (194)	hP12
s21	LiMnAs	P4/nmm (129)	tP6
s22	CaPdSi	$P2_1/c$ (14)	mP12
s23	LaIrSi	$P2_13$ (198)	cP12
s24	La_2Sb	I4/mmm (139)	tI12
s25	LaPtSi	$I4_1md$ (109)	tI12
s26	TiFeSi	Ima2 (46)	oI36
s27	AuEuGe	Imm2 (44)	oI12
s28	ZrRhSn	P-62c (190)	hP18
s29	YPdSi	Pmmn (59)	oP24
s30	FeOCl	Pmmn (59)	oP6
s31	SmSI	R-3m (166)	hR6
s32	ZrO_2	$P2_1/c$ (14)	mP12/Zirconia
s33	NiSSb	$P2_13$ (198)	cP12/Ullmannite
s34	$CoSb_2$	$P2_1/c$ (14)	mP12/Gudmundite
s35	YOF	P4/nmm (129)	tP6
s36	ZrNCl	P-3m1 (164)	hP6
s37	ZrOS	$P2_13$ (198)	cP12
s38	TaON	P6/mmm (191)	hP9
s39	UTe_2	Immm (71)	oI12
s40	Co_2Si	Pnma (62)	oP12
s41	$NiAs_2$	Pbca (61)	oP24/ Pararammelsbergite

transition is considered as forbidden, otherwise allowed. Spin-orbit couplings and excitonic effects are not included in this work.

The power conversion efficiency η of a solar cell is calculated by $\eta = P_m/P_{in}$, where P_{in} is the total incident solar energy density, $P_m = J \times V$ is the maximum output power density. For solar cell illuminated under the photon flux I_{sun} at temperature T that behaves as the ideal diode, the current density J and voltage V follow $J = J_{sc} - J_0(1 - e^{eV/k_BT})$. $J_{sc} = e\int_0^\infty \alpha(E) I_{sun} dE$ is the short-circuit current density, $\alpha(E)$ is the calculated photon absorptivity, E is the photon energy, and e is the elementary charge. $J_0 = J_0^{nr} + J_0^{r} = J_0^{r}/f_r$ is the reverse saturation current consists of nonradiative part J_0^{nr} and radiative part $J_0^{r} = e\pi\int_0^\infty \alpha(E) I_{bb}(E,T) dE$, $f_r = e^{(E_g - E_g^{da})/k_BT}$ is the fraction of the radiative part, E_g is the fundamental bandgap, k_B is the Boltzmann constant, and I_{bb} is the black-body spectrum.

4. Results and Discussions

4.1. Stable Unreported ABX Compounds

The high-throughput approach described above is applied to investigate the 488 unreported ABX with octet electron count (EC = 8) from the groups shown in **Figure 4** to sort the stable versus unstable compounds (shown as green plus and red minus signs in Figure 4, respectively). We predict 235 stable ABX compounds that are not listed in ICSD[11a,11b] or ICDD,[11c] include 1 oxide,[29,30a] 7 sulfides, 6 selenides, 8 tellurides, 9 nitrides, 20 phosphides, 15 arsenides, 18 antimonides, 16 bismides, 14 carbides, 27 silicides, 29 germanides, 29 stannides, and 36 plumbides (see Supporting Information for their crystal structures, formation enthalpies, and optical bandgaps). Five of these compounds are not listed in ICSD[11a,11b] or ICDD[11c] but were synthesized before in the following structures: CuLiS in s1,[30b] AgKTe in s5,[30c] LiMgSb in s1,[30d] AuLaSn in s2,[30e,30f] and LiGaSn in s1 structure.[30g] The ground state structure types found by us for these five materials are in agreement with experiments. Together with the 226 ABX in the groups considered in this paper (Figure 4) that are listed in ICSD[11a,11b] or ICDD,[11c] there are now 461 stable ABX compounds in Figure 4.

We see from Figure 4 that the number of stable nitrides is much smaller than the number of stable phosphides, arsenides, antimonides, or bismides, and the same for carbides compared with silicides, germanides, etc., due to the very stable standard state of nitrogen (N_2 molecule) and carbon (graphite). The strong competition from N_2 molecule and graphite makes the nitrides and carbides have small (negative) formation enthalpies, e.g., NaCdN (–0.07 eV per atom or –6.6 kJ mol^{-1} atom), KCdN (–0.12 eV per atom or –11.8 kJ mol^{-1} atom), NaGaC (–0.08 eV per atom or –7.4 kJ mol^{-1} atom), and CaCdC (–0.22 eV per atom or -21.1 kJ mol^{-1} atom). Small ΔH_f corresponds to small absolute area of the full triangle as illustrated in Figure 3a. The formation enthalpies of the 235 predicted stable ABX compounds are evaluated in the first-principles thermodynamics (see Supporting Information).

4.2. Unstable ABX Used Previously for Property Prediction: The Importance of Thermodynamic Stability Analysis

The hypothetical ABX that are predicted to be unstable with respect to their constituents (235 ones shown as red minus signs in Figure 4) are not likely to be easy to synthesize or to be stable after the synthesis. Out of the ≈600 ABX compounds calculated

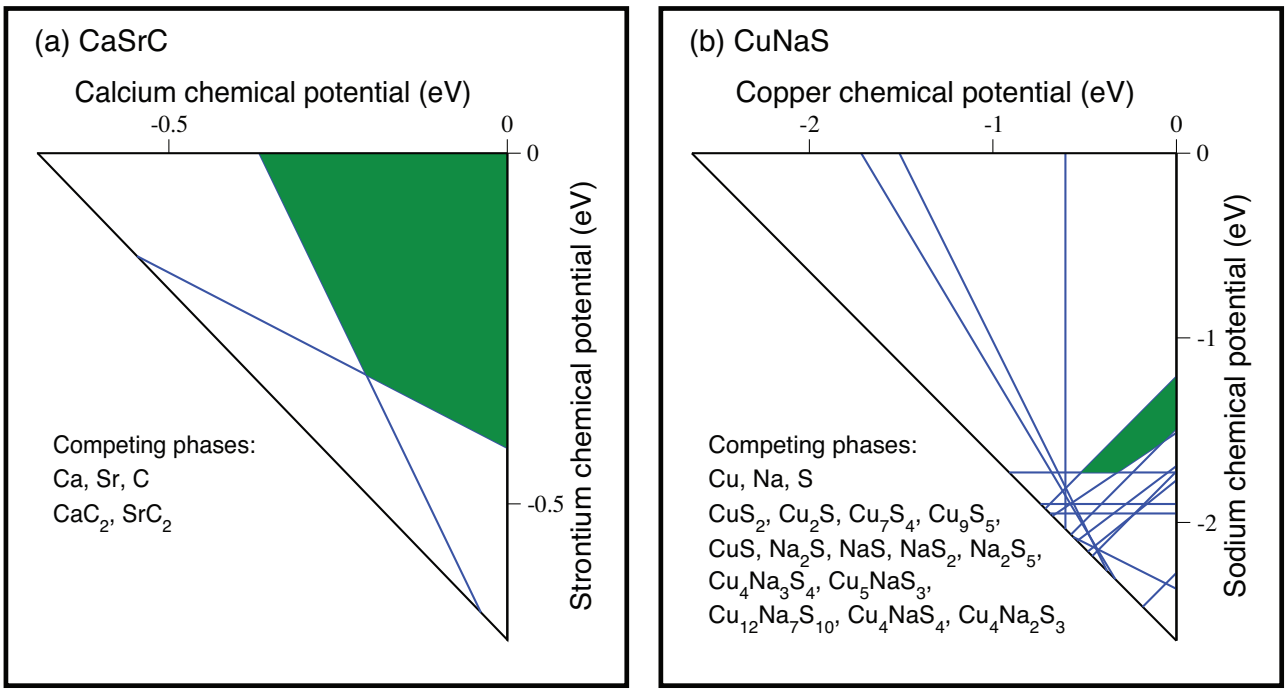

Figure 3. Thermodynamic stability analysis of a) CaSrC and b) CuNaS in the space of chemical potentials of involving elements. The triangle in the 3D chemical potential space is projected to 2D plane.

in presumed single structure prototype in ref. [7a] searching for candidate optoelectronic materials, ≈120 are found by us to be unstable with respect to phase separation. In ref. [4] 15 ABX compounds were suggested as candidate piezoelectric materials, among which two (LiYC and NaScC) are found to be unstable with respect to decomposition in our approach. Additionally, out of the 24 ABX studied in the presumed ZrBeSi-type structure for candidate topological insulators in ref. [5] six compounds (LiAuSe, LiAuTe, LiHgAs, LiHgSb, NaHgAs, and NaAuSe) are found here to be thermodynamically unstable. Overall, the examples presented here illustrate the importance of checking thermodynamic stability with respect to decomposition for proposing new hypothetical compounds with attractive physical properties.

4.3. Structure Diversity of Stable ABX

Figure 5 shows the distribution of the 461 stable ABX compounds (shown in Figure 4) among the ≈40 structure types listed in Table 3. The five most popular structure types are s1 (AgMgAs-type, 44 out of the 461 compounds are in this structure), s2 (LiGaGe-type, 32), s3 (PbClF-type, 57), s5 (ZrBeSi-type, 75) and s6 (MgSrSi-type, 45), which are shown in the inset of Figure 5. Structure s2 is an analog of s1. The former is derived by filling atoms at interstitial sites of wurtzite structure. s26 (TiFeSi-type) is a distorted s4 (Fe2P-type) structure. Structure s5 (ZrBeSi-type) and s17 (BaPtSb-type) structures are both derived from AlB2-type structure. One can see from Figure 5 that less than 10% of the stable compounds are in the s1 structure, which is the presumed prototype used for all hypothetical ABX compounds.[4,7a] Material properties may depend sensitively on the symmetry of the crystal structure. For example, ferroelectricity and Dresselhaus spin splitting can be observed only in non-centrosymmetric structures. It has been noticed[4] that, MgSrSi, MgCaSi, and MgCaGe were reported to exist in the stablest form in the centrosymmetric MgSrSi-type structure, instead of non-centrosymmetric AgMgAs-type structure offered by Roy et al.[4] as candidate ferroelectric materials. AgLiSe and AgNaSe were assigned to be topological insulators in the presumed ZrBeSi-type structure (s5),[5] whereas they are trivial insulators in their corresponding lowest-energy structures,[31] which are s14 and s6 (see Table 3).

We are aware of the fact that metastable materials can sometimes be made, and could exist for long times. The higher-energy structures of the 235 predicted stable ABX compounds are identified in the high-throughput calculations (see Supporting Information). We emphasize that the experimental accessibility of the higher-energy structures reported in the Supporting Information will depend on the energy difference from the lowest-energy structure as well as kinetic barrier preventing the higher-energy structures to relax into lower-energy structures.

4.4. Potential Material Functionalities of the Predicted Stable ABX Compounds

Various functionalities[4,5,7] of the hypothetical ABX compounds in presumed structure were previously proposed based on standard approximations to DFT, which systematically underestimated the bandgaps. Here we calculate instead the physical properties of the new stable compounds in the lowest-energy structure for searching interesting material functionalities, based on GW approximation[13] for electron's self-energy.

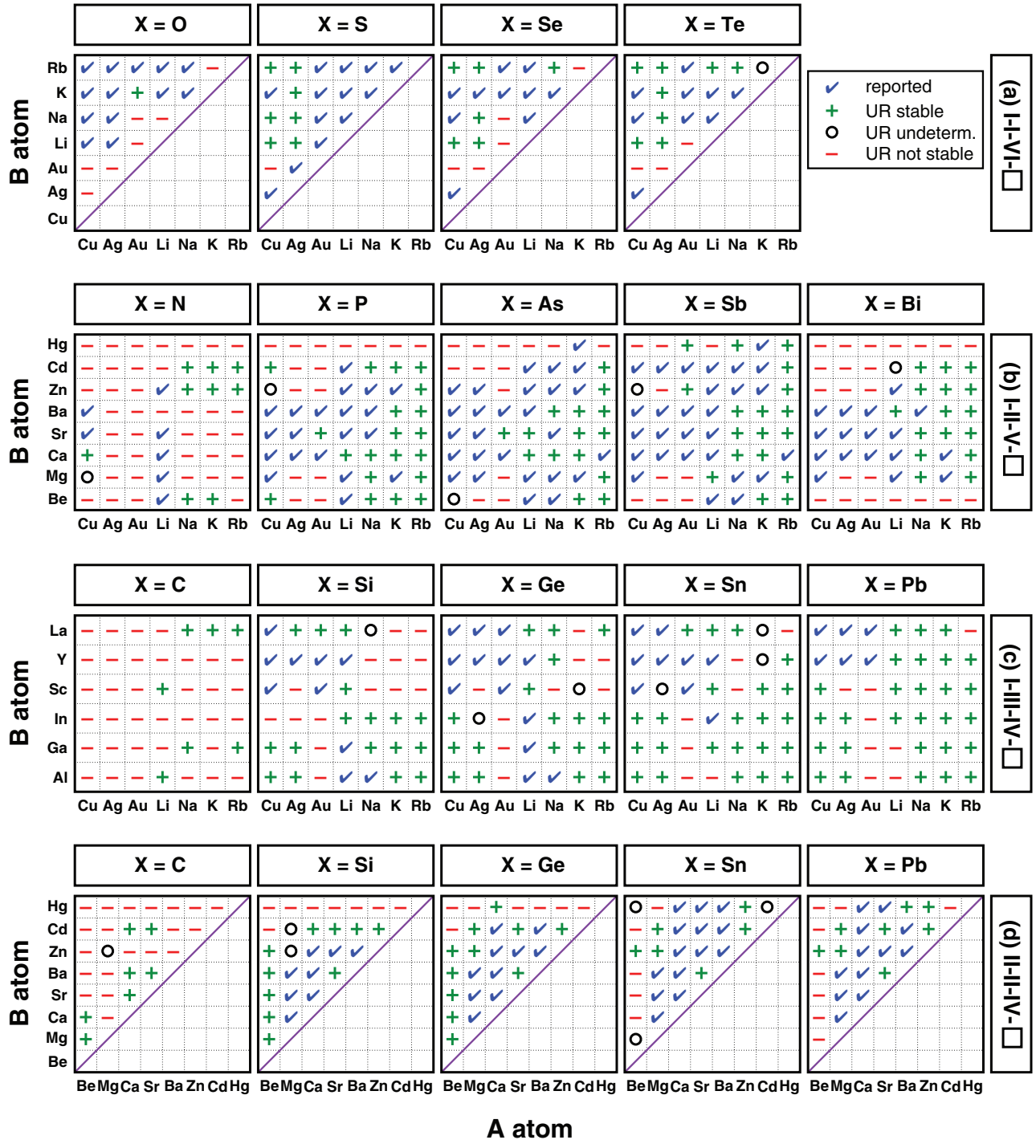

Figure 4. ABX compounds in a) I-I-VI, b) I-II-V, c) I-III-IV, and d) II-II-IV groups. The compounds labeled by check-marks are reported, all others are unreported (UR). Of those, the ones marked by plus are predicted stable, the ones marked by minus are unstable, the ones marked by circle are too close to call (undetermined).

The four optical types (OT1 to OT4) based on three bandgaps, i.e., the indirect bandgap E_g^i, direct optical forbidden gap E_g^{df}, and the direct optical allowed gap E_g^{da}, are illustrated in **Figure 6**. The calculated bandgaps of the predicted stable non-metallic ABX compounds are listed in **Table 4** (see also Supporting Information for all new compounds). Interestingly, we find that a few ABX compounds made of three metals have bandgaps (E_g as the smallest one of E_g^i, E_g^{df}, and E_g^{da}), e.g., SrBaSn (0.82 eV), SrBaPb (0.72 eV), and KScPb (1.62 eV). It is found that there are many compounds with optical type

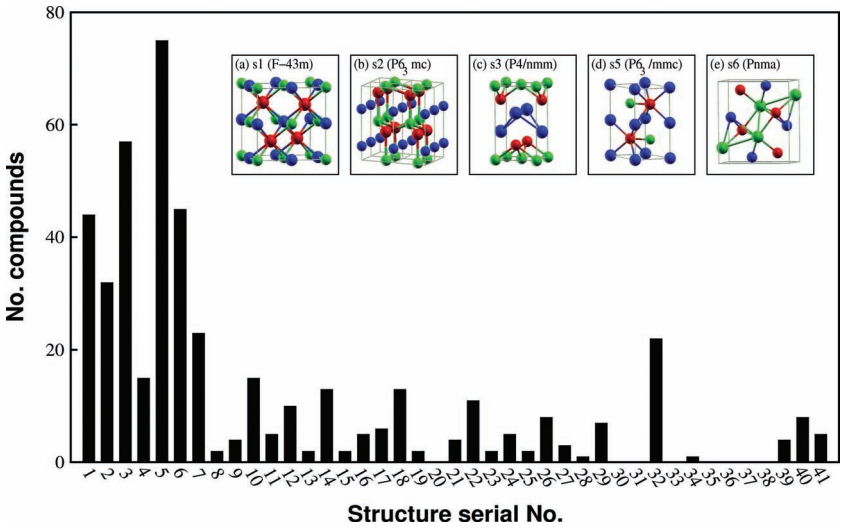

Figure 5. The number of stable ABX compounds in each structure type of 1:1:1 stoichiometry. Inset: The five most popular structure types of ABX compounds with A atom in blue, B in green, and X in red. The structure type is identified via a serial number given in Table 3.

1 and bandgap magnitude ranges from 0.6 eV to 3.3 eV, e.g., KGaGe (0.63 eV), NaCdP (1.01 eV), NaSrSb (1.79 eV), and NaMgP (2.79 eV), residing in the visible light energy range, which may be used for optoelectronics as discussed in ref. [7b] A dozen of ABX compounds have optical allowed bandgaps larger than 3.3 eV, e.g., KZnN (3.65 eV), RbZnN (3.59 eV), AgNaS (4.01 eV), and AgKS (4.73 eV), which are transparent to visible light. We also calculated the spectroscopic limited maximum efficiencies (SLME) for photovoltaics in case of thin-film solar cell with thickness L = 0.5 μm compared to the Shockley–Queisser (SQ) efficiency limit[32] of the predicted stable compounds, which are shown in Figure 6. The calculated SLME of solar cell with L > 0.5 μm is larger than the corresponding value in case of L = 0.5 μm. It is found that dozens of ABX materials having SLME higher than 15%, e.g. LiScC (19.6%), KGaSi (22.9%), SrBaSn(26.1%), and SrBaPb (21.7%), including a few compounds made of three metals, e.g., SrBaSn and SrBaPb.

5. Conclusions

We have examined the 488 unreported ABX compounds from the I-I-VI, I-II-V, I-III-IV, and II-II-IV groups via first-principles thermodynamics. 235 new ABX compounds are predicted to be stable in this paper. Less than 10% of the reported or new stable ABX compounds have the AgMgAs-type crystal structure, which is the presumed prototype used for all hypothetical ABX compounds. 235 out of the 488 unreported compounds are found to be thermodynamically unstable and are not likely to be easily synthesized or to be stable in device structure (for 18 compounds the answers are too close to determine).

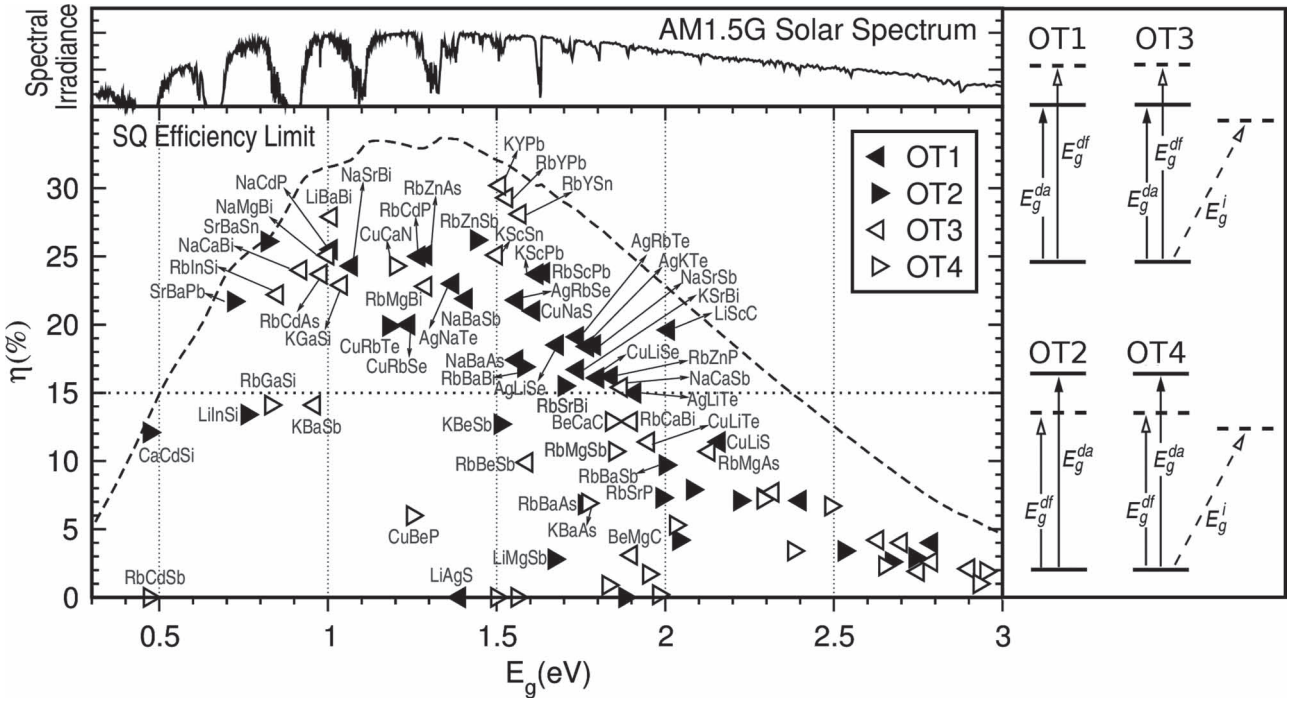

Figure 6. Calculated spectroscopic limited maximum efficiency (SLME) (η) and Shockley-Queisser (SQ) efficiency limit[32] under AM1.5G solar spectrum at T = 300 K for thin-film solar cell of predicted stable ABX materials with thickness of 0.5 μm (left) and schematic illustration of optical types (right) in which electric-dipole allowed (forbidden) direct optical transition is denoted by a line with an arrow pointing to solid (dashed) horizontal line, and indirect states are shown as laterally displaced dashed lines.

Table 4. GW bandgaps (in eV) of the predicted stable non-metallic ABX compounds.

Compd.	E_g^i	E_g^{df}	E_g^{da}	Type	Compound	E_g^i	E_g^{df}	E_g^{da}	Type	Compound	E_g^i	E_g^{df}	E_g^{da}	Type
AuKO	1.50	1.66	2.09	4	RbCaP	2.79	3.07	2.95	3	RbSrBi	–	1.70	1.79	2
CuLiS	–	3.14	2.16	1	RbSrP	–	1.99	2.40	2	RbBaBi	–	1.58	1.67	2
CuNaS	–	1.75	1.61	1	RbBaP	–	2.04	2.56	2	LiAlC	1.95	1.95	2.55	4
CuRbS	1.56	1.75	2.08	4	RbZnP	–	1.93	1.84	1	LiScC	–	2.31	2.01	1
AgLiS	–	1.73	1.39	1	RbCdP	–	1.37	1.27	1	RbGaC	0.33	0.88	0.56	3
AgNaS	–	3.73	4.01	2	AuSrAs	–	0.71	0.19	1	AgAlSi	0.16	0.50	0.51	3
AgKS	3.93	4.36	4.73	4	LiCaAs	2.38	2.41	2.56	4	LiInSi	–	0.76	1.33	2
AgRbS	3.81	4.04	4.61	4	LiSrAs	–	2.08	2.24	2	LiLaSi	0.12	0.24	0.33	4
CuLiSe	–	2.96	1.80	1	NaCaAs	2.49	2.51	2.54	4	KGaSi	1.04	1.53	1.32	3
CuRbSe	–	1.34	1.24	1	NaBaAs	–	2.70	1.56	1	RbAlSi	0.12	0.42	1.64	4
AgLiSe	–	2.34	1.68	1	KBeAs	–	2.67	2.72	2	RbGaSi	0.83	0.88	1.24	4
AgNaSe	–	2.02	1.09	1	KCaAs	2.32	2.54	2.46	3	RbInSi	0.85	1.18	1.09	3
AgRbSe	–	1.71	1.56	1	KSrAs	2.29	2.31	2.39	4	AgAlGe	0.22	0.48	0.41	3
NaRbSe	3.69	4.09	3.74	3	KBaAs	1.77	1.80	2.30	4	KGaGe	–	0.65	0.63	1
CuLiTe	1.95	2.29	2.05	3	RbBeAs	–	2.53	2.54	2	KInGe	0.24	0.34	0.39	4
CuRbTe	–	1.18	1.25	2	RbMgAs	2.13	2.87	2.19	3	RbGaGe	0.21	0.28	0.22	3
AgLiTe	–	2.74	1.91	1	RbSrAs	–	2.22	2.38	2	RbInGe	0.20	0.52	0.28	3
AgNaTe	–	2.05	1.37	1	RbBaAs	–	1.76	2.22	2	AuLaSn	0.18	0.82	0.62	3
AgKTe	–	2.03	1.77	1	RbZnAs	–	1.40	1.29	1	LiScSn	–	0.32	0.23	1
AgRbTe	–	1.95	1.74	1	RbCdAs	0.98	1.55	1.03	3	NaAlSn	0.27	0.34	0.35	4
LiRbTe	3.73	4.48	3.76	3	LiMgSb	–	1.67	2.83	2	NaLaSn	0.41	0.53	0.54	4
NaRbTe	3.52	3.95	3.55	3	NaCaSb	1.87	1.98	1.96	3	KAlSn	0.16	0.67	0.38	3
CuCaN	1.20	1.24	1.33	4	NaSrSb	–	2.23	1.79	1	KInSn	0.14	0.20	0.15	3
NaBeN	2.65	2.68	2.91	4	NaBaSb	–	2.09	1.41	1	KScSn	1.50	1.59	1.53	3
NaZnN	1.83	2.60	3.29	4	KBeSb	–	1.51	1.89	2	RbInSn	0.10	0.17	0.19	4
KBeN	3.49	4.16	3.63	3	KCaSb	2.63	3.08	2.80	3	RbYSn	1.57	1.90	1.61	3
KZnN	1.98	2.17	3.65	4	KSrSb	–	2.44	2.40	1	CuScPb	0.39	0.48	1.17	4
KCdN	0.17	0.43	0.25	3	KBaSb	0.96	2.00	1.26	3	NaLaPb	0.20	0.52	0.41	3
RbZnN	–	1.88	3.59	2	RbBeSb	1.59	1.65	1.61	3	KScPb	–	1.68	1.62	1
CuBeP	1.25	1.47	2.01	4	RbMgSb	1.85	1.90	1.99	4	KYPb	1.51	1.57	1.54	3
CuCdP	–	0.99	0.09	1	RbSrSb	–	2.29	2.40	2	RbGaPb	0.17	0.26	0.25	3
AuSrP	0.28	0.39	0.33	3	RbBaSb	–	2.00	2.21	2	RbInPb	0.20	0.38	0.27	3
LiCaP	2.93	2.98	3.12	4	RbZnSb	–	1.44	1.52	2	RbScPb	–	1.90	1.64	1
NaBeP	2.75	2.96	2.84	3	RbCdSb	0.47	0.50	1.12	4	RbYPb	1.53	1.61	1.54	3
NaMgP	–	3.25	2.79	1	RbHgSb	–	0.60	0.99	2	BeMgC	1.90	3.03	2.60	3
NaCaP	2.95	2.97	3.03	4	LiBaBi	1.01	1.10	1.06	3	BeCaC	1.84	2.03	2.24	4
NaCdP	–	1.84	1.01	1	NaMgBi	1.00	1.53	1.03	3	CaCdSi	–	0.47	0.61	2
KBeP	–	3.31	3.25	1	NaCaBi	0.92	1.80	0.95	3	SrBaSi	–	1.40	0.66	1
KCaP	2.90	3.18	3.04	3	NaSrBi	–	1.67	1.07	1	BeMgGe	0.06	0.10	0.06	3
KSrP	–	2.74	2.85	2	KSrBi	–	1.79	1.74	1	SrCdGe	0.10	0.57	0.39	3
KBaP	2.03	2.06	2.51	4	KBaBi	–	2.26	0.69	1	SrBaSn	–	0.82	0.84	2
RbBeP	–	3.32	3.32	1	RbMgBi	1.29	1.99	1.33	3	SrBaPb	–	0.72	0.84	2
RbMgP	2.70	3.30	2.76	3	RbCaBi	1.90	2.33	2.05	3					

Comparing with the previous studies using assumed crystal structure without thermodynamic analysis, our study emphasizes the importance of checking the lowest-energy structure and thermodynamic stability for an unreported compound before the study of material functionalities. After systematic thermodynamic analysis, we calculated the electronic structures of the

predicted stable compounds in their lowest-energy structures based on GW approximation for electron's self-energy. Remarkably, we find that a few ABX compounds made of three metals with bandgaps of ≈1 eV, whose model photovoltaic efficiencies for $L = 0.5$ μm thin-film solar cell are higher than 15%.

Supporting Information

Supporting Information is available from the Wiley Online Library or from the author.

Acknowledgements

This work was supported by the U.S. Department of Energy, Office of Science, Basic Energy Sciences, Energy Frontier Research Centers, under Contract No. DE-AC36-08GO28308 to NREL. X.Z. also acknowledges the administrative support of REMRSEC at the Colorado School of Mines, Golden, Colorado, and thanks Dr. Stephan Lany, Dr. Haowei Peng, and Dr. Mayeul d'Avezac for helpful discussions. This research used resources of the National Energy Research Scientific Computing Center, which is supported by the Office of Science of the U.S. Department of Energy under Contract DE-AC02-05CH11231 as well as capabilities of the National Renewable Energy Laboratory Computational Sciences Center, which is supported by the Office of Energy Efficiency and Renewable Energy of the U.S. Department of Energy under Contract DE-AC36-08GO28308.

Received: October 22, 2011
Published online: February 3, 2012

[1] a) A. Y. Liu, M. L. Cohen, *Science* **1989**, *245*, 841; b) D. M. Teter, R. J. Hemley, *Science* **1996**, *271*, 53; c) G. K. Pradhan, A. Kumar, S. K. Deb, U. V. Waghmare, C. Narayana, *Phys. Rev. B* **2010**, *82*, 144112.

[2] a) I. I. Oleinik, E. Y. Tsymbal, D. G. Pettifor, *Phys. Rev. B* **2000**, *62*, 3952; b) H. Pan, J. B. Yi, L. Shen, R. Q. Wu, J. H. Yang, J. Y. Lin, Y. P. Feng, J. Ding, L. H. Van, J. H. Yin, *Phys. Rev. Lett.* **2007**, *99*, 127201.

[3] M. Kundu, S. Mahanty, R. N. Basu, *Mater. Lett.* **2011**, *65*, 1105.

[4] A. Roy, J. W. Bennett, K. M. Rabe, D. Vanderbilt, *arXiv* **2011**, 11075078.

[5] H. Zhang, S. Chadov, L. Müchler, B. Yan, X. Qi, J. Kübler, S. Zhang, C. Felser, *Phys. Rev. Lett.* **2011**, *106*, 156402.

[6] S. Froyen, D. M. Wood, A. Zunger, *Phys. Rev. B* **1987**, *36*, 4547.

[7] a) T. Gruhn, *Phys. Rev. B* **2010**, *82*, 125210; b) D. Kieven, R. Klenk, S. Naghavi, C. Felser, T. Gruhn, *Phys. Rev. B* **2010**, *81*, 075208.

[8] a) J. E. Bernard, R. G. Dandrea, L. G. Ferreira, S. Froyen, S.-H. Wei, A. Zunger, *Appl. Phys. Lett.* **1990**, *56*, 731; b) R. G. Dandrea, J. E. Bernard, S.-H. Wei, A. Zunger, *Phys. Rev. Lett.* **1990**, *64*, 36; c) F. Capasso, *Quantum Well and Superlattice Physic II (Spie Vol. 943)*, *Society of Photo Optical* **1988**; d) D. Fischer, M. Jansen, *Angew. Chem. Int. Ed.* **2002**, *41*, 1755; e) L. G. Wang, A. Zunger, *Phys. Rev. Lett.* **2003**, *90*, 256401.

[9] W. Xie, Y. Xu, B. Liu, D. G. Pettifor, *Phys. Rev. Lett.* **2003**, *91*, 037204.

[10] a) E. Gregoryanz, C. Sanloup, M. Somayazulu, J. Badro, G. Fiquet, H. Mao, R. J. Hemley, *Nat. Mater.* **2004**, *3*, 294; b) R. Yu, X. F. Zhang, *Phys. Rev. B* **2005**, *72*, 054103; c) V. Ozoliņš, A. Zunger, *Phys. Rev. Lett.* **1999**, *82*, 767; d) K. Kim, V. Ozoliņš, A. Zunger, *Phys. Rev. B* **1999**, *60*, 8449.

[11] a) G. Bergerhoff, I. D. Brown, in *Crystallographic Databases*, (Eds: F. H. Allen, G. Bergerhoff, R. Sievers), International Union of Crystallography, Chester **1987**; b) A. Belsky, M. Hellenbrandt, V. L. Karen, P. Luksch, *Acta Cryst. B* **2002**, *58*, 364; c) ICDD PDF: International Centre For Diffraction Data, Powder Diffraction File, Newtown Square, PA, USA.

[12] a) G. Hautier, C. C. Fischer, A. Jain, T. Mueller, G. Ceder, *Chem. Mater.* **2010**, *22*, 3762; b) X. Zhang, V. Stevanovi , M. d'Avezac, S. Lany, A. Zunger, unpublished.

[13] a) L. Hedin, *Phys. Rev. A* **1965**, *139*, 796; b) W. G. Aulbur, L. Jönsson, J. W. Wilkins, *Solid State Physics* **2000**, *54*, 1; c) G. Onida, L. Reining, A. Rubio, *Rev. Mod. Phys.* **2002**, *74*, 601.

[14] a) H. Nowotny, W. Sibert, Z. Metall, **1941**, *33*, 391; b) R. Juza, F. Hund, *Naturwissenschaften* **1946**, *33*, 121; c) R. Juza, F. Hund, *Z. Anorg. Chem.* **1948**, *257*, 1; d) H. Nowotny, K. Bachmayer, *Monatsh. Chem.* **1950**, *81*, 488; e) D. M. Wood, A. Zunger, R. de Groot, *Phys. Rev. B* **1985**, *31*, 2570; f) S.-H. Wei, A. Zunger, *Phys. Rev. Lett.* **1986**, *56*, 528. g) D. M. Wood, S.-H. Wei, A. Zunger, *Electronic Structure and Stability of AIBIICV Filled Tetrahedral Compounds*, in Ternary and Multinary Compounds, Proc. 7th Int. Conf. MRS, **1987**, pp. 523–532.

[15] F. Heusler, *Verhandlungen der Deutschen Physikalischen Gesellschaft* **1903**, *5*, 219.

[16] a) J. Yang, H. M. Li, T. Wu, W. Q. Zhang, L. D. Chen, J. H. Yang, *Adv. Funt. Mater.* **2008**, *18*, 2880; b) C. N. Borca, T. Komesu, H. Jeong, P. A. Dowben, D. Ristoiu, Ch. Hordequin, J. P. Noziéres, J. Pierre, S. Stadler, Y. U. Idzerda, *Phys. Rev. B* **2001**, *64*, 052409; c) S. Sakurada, N. Shutoh, *Appl. Phys. Lett.* **2005**, *86*, 082105; d) V. Ksenofontov, G. Melnyk, M. Wojcik, S. Wurmehl, K. Kroth, S. Reiman, P. Blaha, C. Felser, *Phys. Rev. B* **2006**, *74*, 134426.

[17] a) R. Bacewicz, T. F. Ciszek, *Appl. Phys. Lett.* **1988**, *52*, 1150; b) K. Kuriyama, K. Nagasawa, K. Kushida, *J. Cryst. Growth* **2002**, *237*, 2019; c) K. Kuriyama, F. Nakamura, *Phys. Rev. B* **1987**, *36*, 4439; d) K. Kuriyama, T. Katoh, *Phys. Rev. B* **1988**, *37*, 7140; e) K. Kuriyama, T. Kato, K. Kawada, *Phys. Rev. B* **1994**, *49*, 11452; f) K. Kuriyama, T. Ishikawa, K. Kushida, *Phys. Rev. B* **2005**, *72*, 233201.

[18] a) S. Chadov, X. Qi, J. Kübler, G. H. Fecher, C. Felser, S. Zhang, *Nat. Mater.* **2010**, *9*, 541; b) H. Lin, L. A. Wray, Y. Xia, S. Xu, S. Jia, R. J. Cava, A. Bansil, M. Z. Hasan, *Nat. Mater.* **2010**, *9*, 546.

[19] a) G. Trimarchi, A. Zunger, *Phys. Rev. B* **2007**, *75*, 104113; b) G. Trimarchi, A. Zunger, *J. Phys.: Condens. Mater.* **2008**, *20*, 295212; c) G. Trimarchi, A. J. Freeman, A. Zunger, *Phys. Rev. B* **2009**, *80*, 092101; d) X. Zhang, G. Trimarchi, A. Zunger, *Phys. Rev. B* **2009**, *79*, 092102; e) X. Zhang, G. Trimarchi, M. d'Avezac, A. Zunger, *Phys. Rev. B* **2009**, *80*, 241202; f) X. Zhang, A. Zunger, *Phys. Rev. Lett.* **2010**, *104*, 245501; g) X. Zhang, A. Zunger, G. Trimarchi, *J. Chem. Phys.* **2010**, *133*, 194504.

[20] The structure-search with GSGO was performed for structures with fewer than 24 atoms. The population size was set to 64 and the 16 worst individuals were replaced by offspring at each generation. The rate of crossover versus mutation was set to 0.7. A minimum of two independent evolutionary runs with 14 or more generations were performed for each GSGO search.

[21] a) D. M. Deaven, K. M. Ho, *Phys. Rev. Lett.* **1995**, *75*, 288; b) A. R. Oganov, C. W. Glass, *J. Chem. Phys.* **2006**, *124*, 244704; c) A. R. Oganov, J. H. Chen, C. Gatti, Y. Z. Ma, Y. M. Ma, C. W. Glass, Z. X. Liu, T. Yu, O. O. Kurakevych, V. L. Solozhenko, *Nature* **2009**, *457*, 863; d) Y. M. Ma, M. Eremets, A. R. Oganov, Y. Xie, I. Trojan, S. Medvedev, A. O. Lyakhov, M. Valle, V. Prakapenka, *Nature* **2009**, *458*, 182.

[22] We used the Perdew-Burke-Ernzerhof (PBE) exchange-correlation functional[23a,23b] as implemented in the Vienna ab initio simulation package (VASP),[23c] the projector-augmented wave (PAW) pseudopotential,[23d] and energy-cutoff of 220–520 eV. The reciprocal space is sampled using grids with densities of $2\pi \times 0.068$ Å^{-1} and $2\pi \times 0.051$ Å^{-1} for relaxation and static calculation,

respectively. For Cu, Ag, and Au, we used the DFT+U method [23e] and the same U values as in ref. [24].

[23] a) A. Zunger, J. P. Perdew, G. L. Oliver, *Solid State Commun.* **1980**, *34*, 933; b) J. P. Perdew, K. Burke, M. Ernzerhof, *Phys. Rev. Lett.* **1996**, *77*, 3865; c) G. Kresse, J. Furthmüller, *Comput. Mater. Sci.* **1996**, *6*, 15; d) G. Kresse, D. Joubert, *Phys. Rev. B* **1999**, *59*, 1758; e) S. L. Dudarev, G. A. Botton, S. Y. Savrasov, C. J. Humphreys, A. P. Sutton, *Phys. Rev. B* **1998**, *57*, 1505.

[24] V. Stevanović, S. Lany, X. Zhang, A. Zunger, unpublished.

[25] S. M. Woodley, R. Catlow, *Nat. Mater.* **2008**, *7*, 937.

[26] The fitted elemental energies[24] (the values of anionic C, Si, Ge, Sn, and Pb are very close to the total energies calculated from GGA directly, thus the latter are used for simplicity) we used here are shown to improve the calculated formation enthalpies leading to the root-mean-square of 0.07 eV per atom. Correspondingly, we repeated the thermodynamic stability analysis for each compound 10 more times by varying the fitted elemental energy –0.1 to 0.1 eV per atom, and the compounds that can have both stable and unstable answers were labeled by undetermined in our accuracy of method.

[27] S. Lany, *Phys. Rev. B* **2008**, *78*, 245207.

[28] L. Yu, A. Zunger, *Phys. Rev. Lett.* (in press).

[29] The new oxide compound AuKO does not appear in the list of 209 predicted oxides in ref. [30a] since Au element was not considered. Other oxides that were calculated to be unstable in this work also do not appear in the list of stable ternary oxides reported in ref. [30a].

[30] a) G. Hautier, C. C. Fischer, A. Jain, T. Mueller, G. Ceder, *Chem. Mater.* **2010**, *22*, 3762; b) D. Kieven, A. Grimm, A. Beleanu, C. G. F. Blum, J. Schmidt, T. Rissom, I. Lauermann, T. Gruhn, C. Felser, R. Klenk, *Thin Solid Films* **2011**, *519*, 1866; c) W. Bronger, H. U. Kathage, J. Less, *Common Metals* **1990**, *160*, 181; d) A. Beleanu, M. Mondeshki, Q. Juan, F. Casper, F. Porcher, C. Felser, *arXiv* **2011**, 11080584; e) K. Latka, W. Chajec, K. Kmiec, A. W. J. Pacyna, J. Magnetism, *Magnetic Mater.* **2001**, *224*, 241; f) A. Szytula, A. Jezierski, B. Penc, D. Fus, J. Magnetism, *Magnetic Mater.* **2000**, *222*, 47; g) W. Blase, G. Cordier, R. Kniep, Z. Anorg, *Allg. Chem.* **1993**, *619*, 1161.

[31] J. Vidal, X. Zhang, L. Yu, J.-W. Luo, A. Zunger, *Phys. Rev. B* **2011**, *84*, 041109.

[32] W. Shockley, H. J. Queisser, *J. Appl. Phys.* **1961**, *32*, 510.